Interactions of Calf Spleen Purine Nucleoside Phosphorylase with 8-Azaguanine, and a Bisubstrate Analogue Inhibitor: Implications for the Reaction Mechanism

Jacek Wierzchowski[a,*], Agnieszka Bzowska[b], Katarzyna Stępniak[b], and David Shugar[b,c]

[a] Department of Biophysics, University of Warmia and Mazury, 4 Oczapowskiego St., PL-10-719 Olsztyn, Poland. Fax: (48-89)-523-4320. E-mail: jacek.wie@uwm.edu.pl
[b] Department of Biophysics, Institute of Experimental Physics, University of Warsaw, Zwirki and Wigury 93, PL-02-089 Warsaw, Poland
[c] Institute of Biochemistry and Biophysics, Polish Academy of Sciences, 5a Pawinskiego St., PL-02-106 Warsaw, Poland

* Author for correspondence and reprint requests

Z. Naturforsch. **59 c**, 713–725 (2004); received April 19/June 7, 2004

Interactions of calf spleen purine nucleoside phosphorylase (PNP) with a non-typical substrate, 8-azaguanine (8-azaG), and a bisubstrate analogue inhibitor, 9-(2-phosphonylmethoxyethyl)-8-azaguanine (PME-azaG), were investigated by means of steady-state fluorescence spectroscopy. Both 8-azaG and PME-azaG form fluorescent complexes with the enzyme, and dissociation constants are comparable to the appropriate parameters (K_m or K_i) obtained from kinetic measurements. PME-azaG inhibits both the phosphorolytic and synthetic pathway of the reaction in a competitive mode. The complex of 8-azaG with PNP is much weaker than the previously reported Gua-PNP complex, and its dissociation constant increases at pH > 7, where 8-azaG exists predominantly as the monoanion ($pK_a \approx 6.5$). The fluorescence difference spectrum of the PNP/8-azaG complex points to participation of the N(7)H or/and N(8)H tautomers of the neutral substrate, and the 9-(2-phosphonylmethoxyethyl) derivative also exists as a neutral species in the complex with PNP. The latter conclusion is based on spectral characteristics of the PNP/PME-azaG complex, confirmed by fluorimetric determination of dissociation constants, which are virtually pH-independent in the range 6–7. These findings testify to involvement of the neutral purine molecule, and not its monoanion, as the substrate in the reverse, synthetic reaction. It is proposed that, in the reverse reaction pathway, the natural purine substrate is bound to the enzyme as the neutral N(7)H tautomer, which is responsible for the reported strong fluorescence of the guanine-PNP complex.

Key words: Purine Nucleoside Phosphorylase, 8-Azaguanine, Fluorescence Titration

Introduction

Purine nucleoside phosphorylase (PNP, E. C. 2.4.2.1.), a ubiquitous enzyme of the purine salvage metabolic pathway, catalyses the reversible phosphorolysis of purine nucleosides, such as inosine and guanosine, and their 2′-deoxy analogues in eukaryotes and additionally (deoxy)adenosine in some prokaryotes, *e.g. E. coli*, as follows:

$$\beta\text{-(deoxy)nucleoside} + P_i \leftrightarrows \text{purine} + \alpha\text{-(deoxy)ribose-1-phosphate}$$

Mammalian forms of PNP, particularly those of human and bovine origin, have been subjected to extensive structural and kinetic analyses (see Bzowska *et al.*, 2000, and Pugmire and Ealick, 2002 for recent reviews), and the reaction mechanism has been partially elucidated. On the basis of structural (Erion *et al.*, 1997; Mao *et al.*, 1998) and kinetic isotope effect studies (Kline and Schramm, 1995), an oxocarbenium ionic structure of the ribose ring has been proposed for the transition state of the reaction, leading to the development of stable transition state analogues, *viz.* the iminoribitol *C*-nucleosides, referred to as immucillins (Miles *et al.*, 1998; Schramm, 2002; Lewandowicz *et al.*, 2003), which are to date the best PNP inhibitors known, exhibiting promising pharmacokinetic properties (Kicska *et al.*, 2002a). Uncertainty, however, still exists as regards the extent to which the catalytic process of phosphorolysis resembles the well-known acid-catalyzed hydrolysis, *i.e.*, if the process depends on prior nucleoside protonation on the imidazole ring N(7). At least three different mechanistic models have been proposed:

Erion *et al.* (1997), on the basis of site-directed mutagenesis and X-ray crystallography, concluded that no protonation of the purine N(7) occurs, and that the purine ring is negatively charged in the

0939–5075/2004/0900–0713 $ 06.00

transition state, stabilized by a strong hydrogen bond to an asparagine amide (Asn243 in the human enzyme). As a consequence, in the reverse (synthetic) process, the purine base must be bound to the enzyme as an anion, with a negative charge on the imidazole ring. Schramm and coworkers (Fedorov *et al.*, 2001) proposed that, despite the apparent absence of the appropriate acidic amino-acid residue in mammalian forms of PNP, protonation of N(7) can be attained with participation of an activated structural water molecule, thanks to the increased basicity of the nucleoside N(7) when approaching the transition state (cf. Kicska *et al.*, 2002b). This model requires that, in the reverse process, the purine ring must be bound to the enzyme as the neutral N(7)H tautomer. Subsequently, Tebbe *et al.* (1999) modified the Erion model, by postulating a transition state with a negative charge localized on the exocyclic O^6 of the purine moiety, followed by proton transfer from ribose-phosphate to the imidazole ring of the purine base, thus leading to release of a neutral purine molecule.

Although a number of binary PNP-purine and PNP-purine nucleoside complexes have been analyzed by X-ray crystallography (see Bzowska *et al.*, 2000; Pugmire and Ealick, 2002), the resolution attained is inadequate to identify protons. A more recent NMR study of immucillin-PNP complexes (Sauve *et al.*, 2003; Deng *et al.*, 2004), although directly confirming protonation of the iminoribitol N(4′) and the ring N(7) of the immucillin H in the complex, also do not conclusively resolve this problem, since the pyrrolo proton of immucillin is clearly less acidic ($pK_a > 11$, cf. Sauve *et al.*, 2003) than the corresponding purine N(7)H or guanine N(1)H, and has no possibility to tautomerize. It is therefore desirable to directly identify ionic or tautomeric forms of purine substrates and substrate analogues bound to the enzyme.

We have previously demonstrated, in one favorable instance, that the tautomeric form of a bound nucleoside analogue inhibitor of the *E. coli* enzyme (formycin A, a structural analogue of adenosine, and its N^6-methyl derivative) could be identified by means of fluorescence spectroscopy (Kierdaszuk *et al.*, 2000). We here apply similar techniques to analyze complexes of calf spleen PNP with 8-azaguanine, an excellent fluorescent substrate for the reverse synthetic pathway of the reaction (Wierzchowski *et al.*, 1996, 2002), and its 9-(2-phosphonylmethoxyethyl) derivative (Holý *et al.*, 1996), a bisubstrate analogue inhibitor (Kulikowska *et al.*, 1998; Wierzchowski *et al.*, 1999) and a putative transition state analogue for this reaction.

Experimental

Enzyme

Trimeric calf spleen PNP was a product from Sigma (St. Louis, MO, USA). The enzyme was desalted by centrifugation, using HEPES (*N*-2-hydroxyethylpiperazine-*N*′-2-ethanesulfonic acid) buffer as described by Bzowska (2002). Activities of the enzyme preparation were assayed by the standard method (Bzowska *et al.*, 2000) and/or by 7-methylguanosine phosphorolysis at pH 7.0 (Kulikowska *et al.*, 1986). The enzyme concentration was determined from its absorbance at 280 nm, with a molar extinction per monomer of $28.9 \cdot 10^3$ м$^{-1}$cm^{-1} (cf. Bzowska, 2002). Unless otherwise indicated, enzyme concentrations refer to monomer molarity.

Chemicals

8-Azaguanosine (8-azaGuo) was synthesized enzymatically, as previously described (Wierzchowski *et al.*, 1996). 9-(2-Phosphonylmethoxyethyl)-8-azaguanine (PME-azaG), synthesized by Holý *et al.* (1996), was previously reported as an inhibitor of PNP (Kulikowska *et al.*, 1998; Wierzchowski *et al.*, 1999; Wielgus-Kutrowska *et al.*, 2003). Ribose-1-phosphate (R1P), 7-methylguanosine (m^7Guo), and 8-azaG were products from Sigma. The latter was re-crystallized from water as the monosodium salt. All other chemicals were of the highest purity available. Water was filtered through a Milli-Q system (Millipore Corp., USA). Concentrations of stock solutions of substrates, inhibitors and standards, except R1P, were determined spectrophotometrically, using molar extinctions listed in Table I.

Instrumentation

Spectrophotometric measurements were carried out with Kontron (Austria) Uvikon-922, Uvikon-930 or Shimadzu UV-1601PC instruments, equipped with thermostatic units. Fluorescence was measured with a Shimadzu RF-5001PC or a Perkin-Elmer LS-50B spectrofluorimeter (Norwalk, CT, USA), both with thermostatically-controlled cell compartments. Spectral bandwidths were 2–

5 nm for the entrance slit, and 3–15 nm for the exit slit.

Enzyme kinetics

Phosphorolysis of m^7Guo was followed spectrophotometrically at 260 nm (Kulikowska *et al.*, 1986). Rates of enzymatic synthesis of 8-azaGuo were measured either spectrophotometrically, with observation at 260 nm and $\Delta\varepsilon$ determined at each pH ($6.5 \cdot 10^3$ M^{-1}cm^{-1} at pH 7.0), or fluorimetrically, using the purified product (8-azaGuo) as an internal standard (Wierzchowski *et al.*, 2002). In the latter case the reaction rates were calculated according to the formula:

$$v = \frac{dF}{dt}\frac{c_{st}}{F_{st}}$$

where *dF/dt* is the fluorescence change with time, F_{st} the fluorescence of the standard, c_{st} the concentration of the standard.

For kinetic measurements employing high substrate concentrations, corrections for the inner-filter effect were introduced, by multiplying the resultant rates by $10^{A/2}$, where A is the absorbance of the sample at the excitation wavelength, as determined spectrophotometrically prior to fluorimetric measurements. At pH < 6.5, where 8-azaGuo is virtually nonfluorescent, the synthetic reaction was followed by the decrease in fluorescence of the neutral form of the substrate (8-azaG) at 420 nm with excitation at 315 nm, the initial fluorescence signal serving as an internal standard for rate calculations. All assays and kinetic measurements were carried out at 25 °C.

Kinetic parameters were calculated with the use of linear multiple regression analysis, by fitting the initial rate data to the generalized kinetic equation for a bisubstrate enzymatic reaction in the form (Segel, 1975):

$$\frac{V_{\max}}{V} = 1 + \frac{K_{m1}}{[S_1]} + \frac{K_{m2}}{[S_2]} + \frac{K_{12}}{[S_1][S_2]} \qquad \{1\}$$

where V and $V_{\max}$ are actual and maximal initial rates, $[S_1]$ and $[S_2]$ concentrations of the two substrates, K_{m1} and K_{m2} the Michaelis constants in μM, and K_{12} the mixed constant in μM^2. Constants K_{m1}, K_{m2}, and K_{12} were fitted as independent parameters.

Inhibition of the enzyme by the bisubstrate analogue inhibitor PME-azaG was analyzed assuming a double competitive model (*i.e.*, assuming only a binary enzyme-inhibitor complex):

$$\frac{V_{\max}}{V} = 1 + \frac{K_{m1}}{[S_1]} + \frac{K_{m2}}{[S_2]} + \frac{K_{12}}{[S_1][S_2]}\left(1 + \frac{[I]}{K_i}\right) \qquad \{2\}$$

where $[I]$ is the inhibitor concentration and K_i the inhibition constant. With one of the substrates (S_2) at constant concentration, it is possible to determine the apparent inhibition constants, K_i^{app}, by measuring initial rates with varying concentrations of the second substrate (S_1) and the inhibitor. The thermodynamic value of the inhibition constant K_i is related to K_i^{app} by:

$$K_i^{app} = K_i\left(1 + \frac{[S_2]}{K_{m2}}\right) \qquad \{3\}$$

Fluorimetric titrations

Fluorimetric titrations were performed in 1-ml semi-micro cuvettes with a 4-mm pathlength in the excitation beam. In some experiments, enzyme concentration was kept constant during titration (*i.e.*, the titrant additionally contained protein at a concentration equal to that in the titrated sample). Otherwise, corrections for enzyme dilution were introduced. Fluorescence intensity was always corrected for the inner-filter effect.

Titration curves, $F(X)$, where X is the total ligand concentration, were fitted nonlinearly to a single binding site model, which leads to the following equation (Kierdaszuk *et al.*, 2000):

$$F - F_0 = F_L X + F_p\left[X + E + K_d - \sqrt{(X + E + K_d)^2 - 4XE}\right]/2 \qquad \{4\}$$

where K_d is the dissociation constant, E the concentration of binding sites, F_0, F_L and F_p are the fluorescence intensities of free protein, free ligand and protein-ligand complex, respectively. When results are expressed in terms of difference spectra ($F - F_{sum}$), the titration curves are expressed as:

$$F - F_{sum} = F_p\left[X + E + K_d - \sqrt{(X + E + K_d)^2 - 4XE}\right]/2 \qquad \{5\}$$

and for those cases where $E << X$, the above equation is simplified to (Kierdaszuk *et al.*, 2000):

$$F - F_{sum} = \frac{F_p}{1 + K_d / X} \qquad \{6\}$$

Results and Discussion

Spectral properties of 8-azaG, PME-azaG and 8-azaGuo

Spectral properties of 8-azaG and 8-azaGuo, reported previously (Wierzchowski *et al.*, 1996), are summarized in Table I and Fig. 1, and compared to those of PME-azaG. It is evident that UV and fluorescence spectra of the PME-azaG fluorophore with either the neutral or monoanionic form of the base moiety (cf. Fig. 2) are virtually identical to the corresponding spectra of 8-azaGuo, but quite distinct from those of 8-azaG. In general, the monoanionic forms of these two compounds are highly fluorescent, while their neutral forms emit only weakly. The reverse holds for 8-azaG (Table I). The higher pK_a for deprotonation of PME-azaG relative to 8-azaGuo (9.0 *vs.* 8.0) is ascribed to electrostatic interactions with the ionized phosphonate group (p$K_a \approx 7.7$). For both compounds pK_a values determined spectrophotometrically were in good agreement with those obtained from fluorimetric titrations.

These striking differences in spectral properties between 8-azaG and its nucleoside are attributed to structural differences between their neutral, as well as their monoanionic forms. As demonstrated previously (Wierzchowski *et al.*, 1996), neutral 8-azaG exists as a mixture of at least two tautomeric forms, one of which, minor, exhibits intense fluorescence at 395 nm, while the dominant N(9)H form is virtually nonfluorescent, leading to striking differences between the UV absorption and fluorescence excitation spectra (see Fig. 1a). The fluorescent tautomer has been tentatively identified as N(8)H, albeit minor participation of the N(7)H form cannot be excluded. This tautomerism is not possible in the nucleoside, nor in the 9-alkoxyphosphonate derivative.

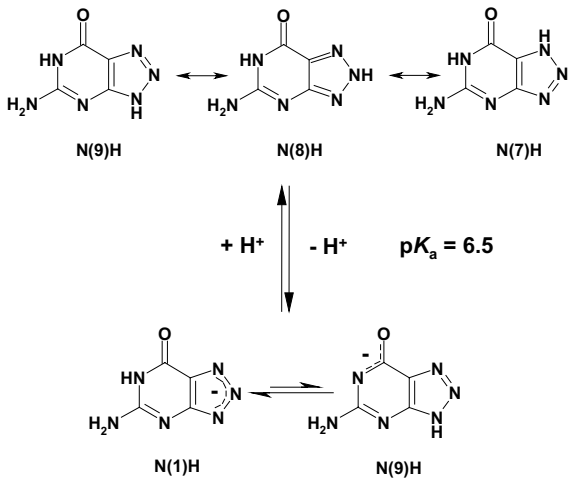

Scheme 1. Postulated tautomerism of 8-azaguanine in its neutral (upper) and monoanionic (lower) forms. Note that the N(9)H form of the monoanion exists to only a small extent, about 3% (see text for details).

The difference between the monoanion structures of 8-azaG and 8-azaGuo is a consequence of the high acidity of the triazole proton in the former compound, generally true for 8-azapurines (Albert, 1986). While the monoanion of 8-azaGuo (pK_a 8.0) resembles that of Guo, *i.e.*, it results form dissociation of the N(1)H, the parent base, 8-azaG, tends to lose the more acidic triazole proton (pK_a 6.5), as shown in Scheme 1. This conclusion is supported by comparison of the pK_a values for proton dissociation of the *N*-methyl derivatives of 8-azaG which, for the N(9), N(8) and N(7) methyl congeners, are in the range 8.0–8.65 (Albert, 1986; Wierzchowski *et al.*, 1996), *i.e.*,

Table I. Spectral parameters for neutral and monoanionic forms of 8-azaG, 8-azaGuo, and PME-azaG. Data from Albert (1986), Wierzchowski *et al.* (1996, 2002), Holý *et al.* (1996), and present work.

Compound (pH)	pK_a	UV absorption		Fluorescence	
		λ_{max} [nm]	ε_{max} [$M^{-1}cm^{-1}$]	λ_{max} [nm]	ϕ
8-azaG (4.5)	6.5, 10.8	249	11200	395	0.33[a]
8-azaG (8.9)		278	6200	355	0.03
8-azaGuo (6.0)	8.05	256	12900	347	< 0.01
8-azaGuo (10.2)		278	11700	360	0.55
PME-azaG (4.5)	9.05	253	12000	350	~ 0.01
PME-azaG (11.2)		278	11200	360	0.38

[a] Determined with excitation at 315 nm (Wierzchowski *et al.*, 1996). Other ϕ values are virtually independent of λ_{exc}.

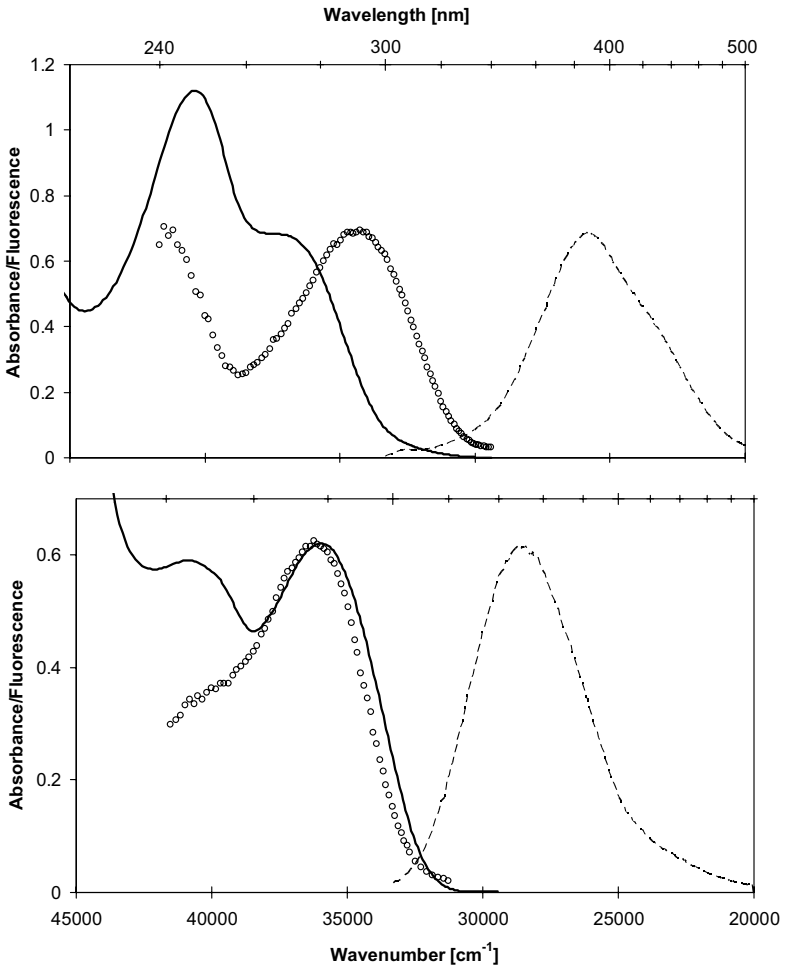

Fig. 1. Spectral properties of the neutral form of 8-azaG at pH 4.5 (upper frame) and of the monoanion at pH 8.9 (lower frame): (———) absorption spectra, 100 μM; (– – –) emission specta with λ_{exc} = 290 nm; (○○○○○) fluorescence excitation spectra, corrected and normalized to the absorption spectra.

1.5 to 2.2 units above the pK_a for the parent 8-azaG.

Since pK_a values for proton dissociation for 8-azaG and 8-azaGuo differ by only 1.5 units, it is plausible that a small proportion (~ 3%) of the "classic" structure N(9)H, *i.e.* resulting from dissociation of the N(1)H, may be present in the 8-azaG monoanion. We have examined the fluorescence excitation spectrum of 8-azaG at pH ~ 9 and found that it differs significantly from the UV absorption spectrum (cf. Fig. 1b, note especially the absence of the second maximum at ~ 245 nm in the excitation spectrum), but fits very well to both the UV absorption and fluorescence excitation spectra of 8-azaGuo (or PME-azaG, see Fig. 2) monoanion. It is therefore very likely that the observed weak emission of the 8-azaG monoanion at pH 9, centered at 355 nm (see Table I), originates from the minor N(9)H structure, while the principal N(1)H form, with negative charge localized on the triazole ring, must be regarded as virtually nonfluorescent.

8-azaG and 8-azaGuo as fluorescent/fluorogenic substrates for calf spleen PNP

8-azaG, a fluorescent analogue of guanine, has been previously shown to be a good and, in some conditions (pH > 7), a highly fluorogenic substrate for the calf spleen, as well as the human PNP in the reverse synthetic pathway (Wierzchowski *et al.*, 2002).

We have reevaluated kinetic parameters for this reaction at various pH values, using desalted enzyme (Bzowska, 2002) and phosphate-free buffers.

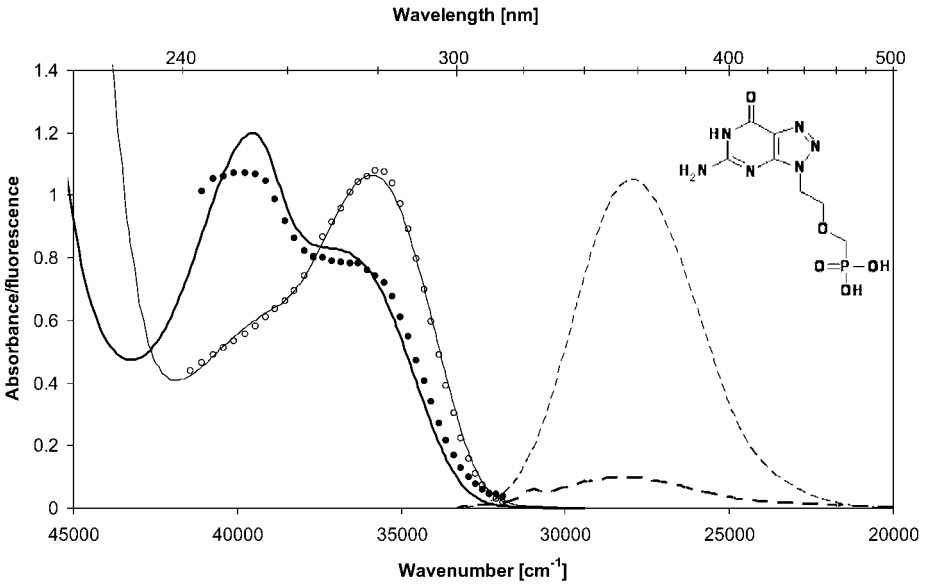

Fig. 2. UV absorption, fluorescence emission (λ_{exc} = 290 nm) and fluorescence excitation spectra of PME-azaG: Neutral form at pH 4.5: (———) UV absorption; (– – –) emission (× 10); (●●●●) fluorescence excitation. Monoanion at pH 11.2: (———) UV absorption; (- - - - -) emission, normalized to UV absorption; (○○○○) fluorescence excitation.

The fluorimetric method was used to determine initial velocities and spectrophotometric measurements to check the reaction rates at various pH. The initial velocity data were fitted to the generalized kinetic equation (eqn. {1}, see Experimental), using multiple regression. The resulting kinetic parameters (K_{m1}, K_{m2}, K_{12} and V_{max}), obtained using the UV and/or fluorimetric methods, are shown in Table II. The observed strong pH-dependence of K_m, but not V_{max}, suggests that only the neutral form of 8-azaG (pK_a 6.5) is a substrate in the synthetic reaction. This is in qualitative agreement with previous, preliminary data (Wierzchowski *et al.*, 1996), as well as with a more detailed analysis of the human enzyme (Wierzchowski *et al.*, 2002). There is also apparently no synergistic interaction between binding sites for both substrates, since $K_{12} \approx K_{m1} \cdot K_{m2}$, especially pronounced at pH 7 to 8.

Reversibility of the reaction and equilibrium constant

The enzymatic synthesis of 8-azaGuo, previously regarded as virtually irreversible (Wierzchowski *et al.*, 1996), is, in fact, reversible, but its estimated equilibrium constant, K_{eq} ~ 320, is highly in favor of nucleoside synthesis compared to the natural purines (K_{eq} ~ 55). We have also noted that the

Table II. Kinetic parameters for synthesis of 8-azaGuo from 8-azaG and R1P, catalyzed by calf spleen PNP, reevaluated using multiple regression analysis. The parameters were obtained by fitting initial velocity data to equation {1} (see Experimental).

pH[a]	V_{max} relative	K_m (8-azaG) [μM]	K_m (R1P) [μM]	K_{12} [μM^2]	r^2
8.06[a]	0.94	~ 680	265	$1.7 \cdot 10^5$	0.995
6.97[a]	1.02	101	52	$4.8 \cdot 10^3$	0.999
6.15[a]	0.99				
5.89[b]		91	65	$1.96 \cdot 10^3$	0.992

[a] HEPES buffer, [b] acetate/NH_3 buffer, both at 40 mM.

phosphorolysis of 8-azaGuo with calf PNP is about 150-fold slower than for guanosine, and under standard experimental conditions employed for PNP kinetics it is barely detectable. The K_m value for 8-azaGuo phosphorolysis in 50 mM phosphate buffer, pH 7.0, was found to be ~ 55 μM (data not shown), of the same order of magnitude as that for guanosine (~ 13 μM).

Inhibition of PNP by PME-azaG

Some 9-alkoxyphosphonoethyl purines and purine analogues, previously examined as PNP inhibitors in the phosphorolytic pathway (Kulikowska *et al.*, 1998; Wierzchowski *et al.*, 1999; Wielgus-Kutrowska *et al.*, 2003), exhibited competition with both nucleoside and phosphate substrates (Kulikowska *et al.*, 1998). We now present a more detailed analysis of PME-azaG as an inhibitor of both the phosphorolytic and synthetic pathway.

In the phosphorolytic pathway, the substrate employed was *N*(7)-methylguanosine (m^7Guo) which, in striking contrast to Ino and Guo, fairly well follows Michaelis-Menten kinetics (Bzowska, 2002). With fixed concentrations of one substrate (nucleoside or phosphate), apparent inhibition constants (K_i^{app}) were calculated from initial velocity data with variable concentrations of the inhibitor and the second substrate. Dixon plots displayed a competitive mode of inhibition (not shown), but the apparent K_i values were dependent on the fixed substrate concentration (cf. Fig. 3). In accordance with equation {3}, plots of K_i^{app} *vs.* fixed substrate concentrations were linear in the concentration range 0.1–5 mM for phosphate and 20–300 μM for m^7Guo, giving intercepts of 0.70 ± 0.28 μM for P_i and 0.98 ± 0.21 μM for m^7Guo as fixed substrates, respectively. However, the recorded slopes, $4.6 \cdot 10^{-3}$ for m^7Guo and $6.9 \cdot 10^{-3}$ for phosphate, do not correspond to the expected values of K_i/K_m, which are ~ 0.06 for m^7Guo (disagreement by a factor of 13) and ca. 0.01–0.02 for phosphate (Kulikowska *et al.*, 1986; Bzowska, 2002). Thus, the apparent inhibition constants are somewhat less sensitive to the m^7Guo concentration, *i.e.*, at nearly saturating levels of m^7Guo, K_i^{app} values remain close to the thermodynamic K_i value. We conclude that inhibition of the phosphorolytic reaction by PME-azaG, with K_i = 0.8 ± 0.2 μM at pH 7, is not strictly represented by the competitive model of inhibition, based on Michaelis-Menten kinetics. The marked increase in K_i at pH 8 (data not shown), is clearly due to the effect of secondary phosphonate ionization, bearing in mind that the pK_a of benzyl phosphonate is 7.7.

In turn, we examined the inhibition of the reverse synthetic reaction by PME-azaG, with 8-azaG and ribose-1-phosphate (R1P) as substrates in phosphate-free HEPES buffer, pH 7. As for the phosphorolytic pathway, an apparently competitive type of inhibition was observed (data not shown), and the K_i^{app} values were markedly dependent on the second (fixed) substrate concen-

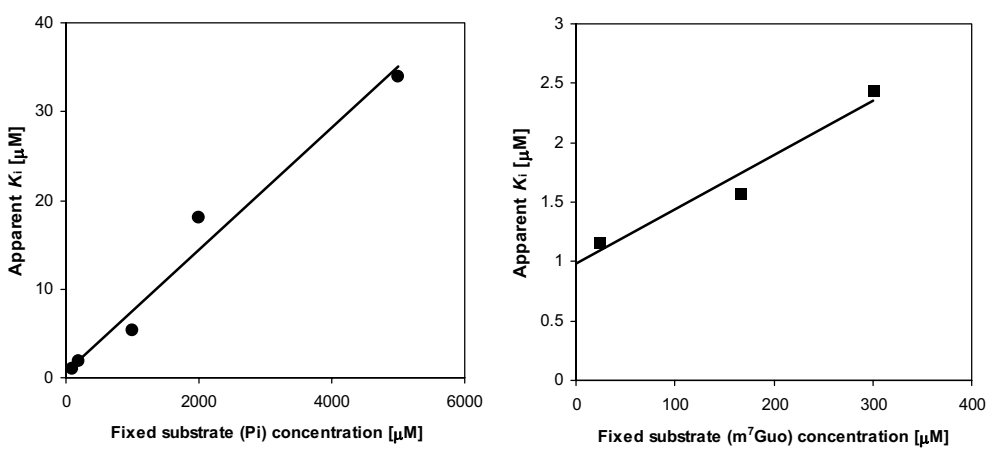

Fig. 3. Determination of the inhibition constant (K_i) of PME-azaG for inhibition of m^7Guo phosphorolysis by calf spleen PNP at pH 7. Left panel: Apparent K_i, obtained from Dixon plots (not shown) of inhibition at constant phosphate concentrations, and variable inhibitor and m^7Guo concentrations. Right panel: Analogous data obtained at variable inhibitor and P_i concentrations, with constant m^7Guo concentration. Y-intercepts are 0.70 ± 0.28 μM for P_i, and 0.98 ± 0.21 μM for m^7Guo as fixed substrates, respectively.

Fixed substrate	Concentration [μM]	Variable substrate	K_i^{app} [μM]	Calculated K_i [μM]
R1P	190	8-azaG	9.16	2.06
R1P	40	8-azaG	2.82	1.63
8-azaG	317	R1P	7.17	1.72
8-azaG	40	R1P	3.20	2.29

Table III. Inhibition constants, at pH 7 and 25 °C, for PME-azaG inhibition of calf spleen PNP in the reverse synthetic pathway, with 8-azaguanine (8-azaG) and α-D-ribose-1-phosphate (R1P) as substrates.

tration. The calculated values of K_i (1.9 ± 0.3 μM, cf. Table III), obtained assuming a "double-competitive" model of inhibition (equations {2} and {3}), were in this case virtually independent of the fixed substrate concentration, thus fully consistent with competition of PME-azaG with both 8-azaG and R1P. But the observed disagreement between the K_i values for the phosphorolytic and synthetic pathways points to more complex enzyme-inhibitor interaction. Similar, or even larger, discrepancies have been noted for other PNP inhibitors (J. Wierzchowski, unpublished data).

Binary complex between PNP and 8-azaG

Guanine forms a tightly bound ($K_d < 1$ μM), and highly fluorescent complex with calf spleen PNP in phosphate-free media (Porter, 1992; Bzowska, 2002). The origin of this fluorescence, initially ascribed to formation of the guanine monoanion upon binding (Porter, 1992), is difficult to interpret, since fluorescence of the complex, centered at ~ 330 nm, coincides with the protein emission. We therefore attempted to characterize the analogous complex with the fluorescent 8-azaG. Best results were obtained with excitation at 310–315 nm, where both protein and ligand have relatively weak absorbances. At pH 7 and with ligand concentrations of ~ 100 μM, a relatively strongly fluorescent complex can be observed, with fluorescence emission centered at 370 nm, resembling somewhat that of neutral 8-azaG (395 nm), but with at least a 20-fold higher intensity (cf. Fig. 4). A titration curve (Fig. 4, right panel), analyzed using the standard equation for single-site binding (equation {6}, see Experimental), led to an association constant of 90 ± 5 μM, a value close to the K_m obtained from kinetic measurements (cf. Table II). Similar results were obtained at pH 7.7, but the fitted association constant was higher, ~ 450 μM (not shown), again in line with kinetic data. Thus, K_d for the complex between 8-azaG and PNP is at least 2 orders of magnitude higher than for the analogous guanine/PNP complex.

With excitation at 290 nm and after subtracting the spectrum of the free ligand (Fig. 4), both protein and bound ligand emission can be observed separately at 320–330 and 370 nm, respectively. Under these conditions, protein fluorescence is virtually unchanged during titration (see Fig. 4), in apparent contrast to the guanine/PNP binary complex (Porter, 1992), but resembling our previous data on PNP complexes with alkoxyphosphonate derivatives of guanine (Wierzchowski *et al.*, 1999). Taken together, these data give further credence to our interpretation of the fluorescence enhancement in the guanine/PNP complex (Porter, 1992) as originating from the purine moiety (possibly in an ionic and/or non-typical tautomeric form, cf. Wielgus-Kutrowska *et al.*, 2002), and not from protein tryptophan.

The increase of 8-azaG fluorescence upon binding PNP and its shift from 395 to 370 nm can be interpreted either in terms of fluorescence enhancement upon binding or as the effect of a tautomeric shift, as previously found for tautomerizable nucleoside analogue inhibitors bound to *E. coli* PNP (Kierdaszuk *et al.*, 2000). Comparison of the fluorescence of the 8-azaG/PNP complex with that of free 8-azaG at pH 8.9 (Table I, Fig. 1) strongly suggests that this emission is unlikely to originate from the fluorescent 8-azaG anion, which emits at 355 nm in aqueous medium, since this would imply an increase of the Stokes' shift by 15 nm in the complex, contrary to the usual decrease in the Stokes' shift observed for fluorescent ligands upon binding to the PNP active site (Wierzchowski *et al.*, 1999, and unpublished data). For the same reason the principal N(9)-H tautomer of neutral 8-azaG, which emits at ~ 350 nm, is excluded (cf. Table I and Fig 2). Hence the most likely source of the strong emission of the complex at 370 nm is the neutral N(8)H or/and N(7)H tautomer of 8-azaG.

The difference UV absorption spectrum, recorded during titration, is close to a "mirror image" spectrum of the neutral to anion transition

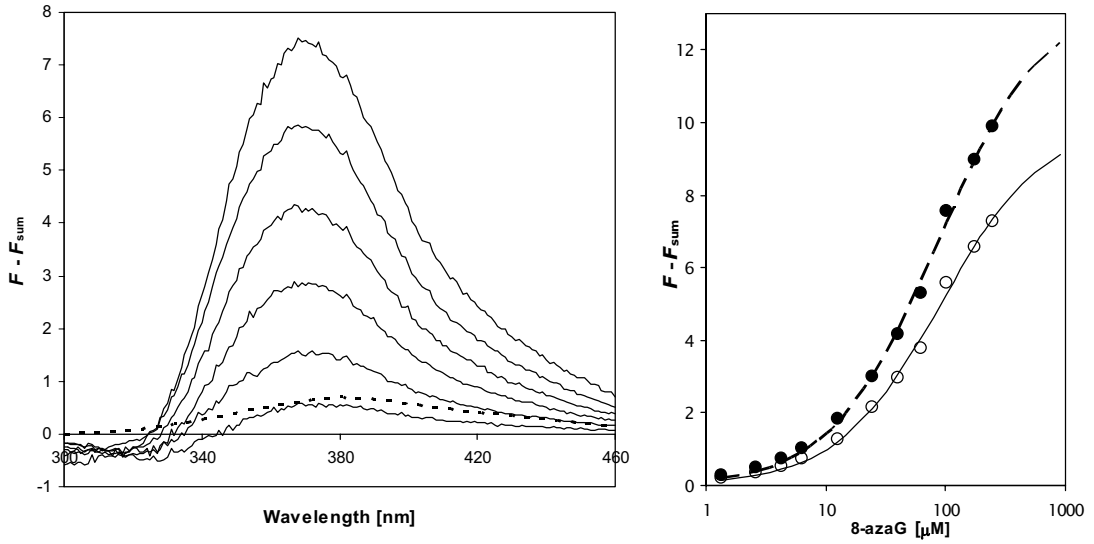

Fig. 4. Left panel: Fluorimetric titration of calf spleen PNP (13.9 μM as monomer, and kept constant) with 8-azaG at pH 7. Shown are difference spectra with λ_{exc} 290 nm and 8-azaG concentrations (from bottom to top curve) of 5.1, 12.5, 24.6, 40.3, 62.8 and 101 μM; (- - - -) fluorescence emission of free 13.9 μM 8-azaG, for comparison.
Right panel: Fluorimetric titration of calf spleen PNP (5.9 μM as monomer) with 8-azaG in 20 μM HEPES, pH 7, with λ_{exc} 315 nm, and fluorescence emission monitored at 370 nm (●●●●) and 390 nm (○○○○). Theoretical curves correspond to K_d values of 92 and 85 μM, respectively.

(Fig. 5). Bearing in mind that, at pH 7, 8-azaG is largely (~ 70%) in the anionic form, this result additionally supports the proposal that the ligand is bound in its neutral form, with a possible tautomeric shift towards the strongly fluorescent N(7)H or/and N(8)H forms.

Taken together, both the kinetic and spectral data argue against binding of anionic 8-azaG as the starting point in the reverse synthetic reaction of PNP, as postulated by Erion *et al.* (1997) for natural purines. It should be noted, in this context, that the anionic form postulated in Erion's mecha-

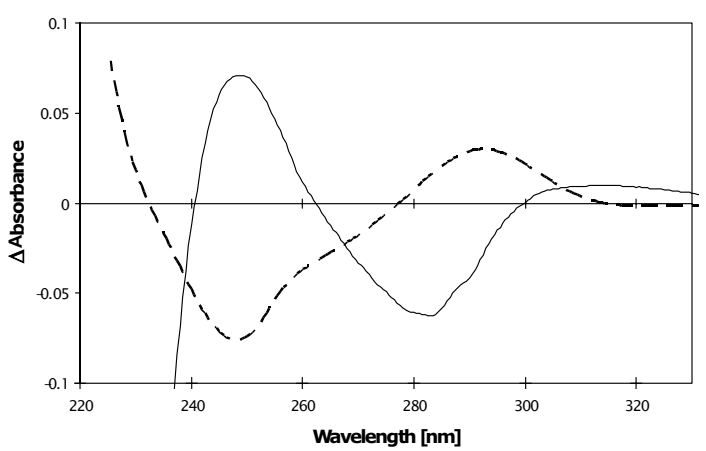

Fig. 5. (———) UV difference spectrum, in 20 mM HEPES, pH 7, between calf spleen PNP (13.9 μM) + 8-azaG (67 μM) and the sum of the two constituents; (– — — —) calculated difference spectrum between the anionic and neutral forms of 8-azaG (13.9 μM). Note the approximate mirror images of the two curves.

nism (*i.e.*, deprotonation of the imidazole ring) does not correspond to the predominant anionic form of guanine or hypoxanthine, involving dissociation of the N(1)-H (Shugar and Psoda, 1991), but does correspond to that of the 8-azaG anion, resulting from dissociation of the triazole proton (Scheme 1; cf. Albert, 1986). If binding of this anionic species is really the starting point of the reaction, one would expect its strong association to the enzyme, which is not the case. Thus, the observed relatively weak binding of 8-azaG and no evidence for an anionic structure in its complex with PNP argue against the Erion model and is in favor of a model involving the neutral purine species as the substrate in the synthetic pathway.

Binary complex between PNP and PME-azaG

Desalted calf spleen PNP, 3–11 μM, was titrated with the title compound at pH 7 and 5.9, with excitation at 290 nm or 305 nm. Spectral effects of titration and a typical titration curve are given in Fig. 6. Fluorescence difference spectra reveal in all cases a fairly strong complex, emitting at 340 nm, *i.e.*, clearly different from that obtained for the PNP complex with 8-azaG (~370 nm, see Fig. 3). This is because PME-azaG (as well as 8-azaGuo) does not display a ring prototropic tautomerism, thus spectrally resembling the principal N(9)H form of 8-azaG.

Nonlinear fitting of the titration curve to equation {5} (see Experimental) revealed essentially a single binding site and an association constant, $K_d \approx 0.4\,\mu$M at pH 5.9 and 0.55 μM at pH 7, slightly lower than that previously reported (Wierzchowski *et al.*, 1999), possibly due to better desalting of the enzyme. This value is somewhat lower than the inhibition constant, K_i (see above), suggesting that the assumed one-site model of inhibitor binding and/or the Michaelis-Menten kinetic model may not be strictly applicable.

The stoichiometry of complexes of PNP with purine alkoxyphosphonates has been the subject of some uncertainty (Wierzchowski *et al.*, 1999; Bzowska, 2002). On the basis of titration curves, we previously postulated a 1:3 (or one per trimer) stoichiometry (Wierzchowski *et al.*, 1999), similar to that reported for transition-state analogues (Miles *et al.*, 1998). Some doubts remain, however, as to whether enzyme concentration, determined from UV absorption at 280 nm, corresponds strictly to the active site concentration. Different enzyme preparations do not give fully reproducible results, undoubtedly related to the fact that their specific activities differ markedly from the reported maximum value of 34 U/mg (Bzowska *et al.*, 2000). In the present case, with a specific activity of the enzyme of 14 U/mg, an apparent stoichiometry close to 1:2 was obtained. We therefore conclude that the most likely stoichiometry of the PME-azaG/PNP complex is 1:1 (*i.e.* three molecules of inhibitor per trimeric enzyme; cf. Bzowska, 2002; Iwanow *et al.*, 2003).

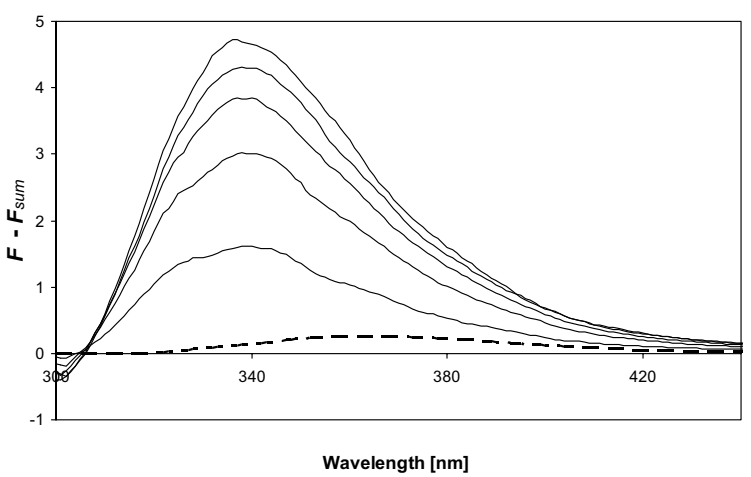

Fig. 6. Fluorimetric titration of calf spleen PNP (11.9 μM as monomer, kept constant) with the inhibitor PME-azaG in phosphate-free acetate buffer at pH 5.9. Difference spectra recorded at inhibitor concentrations (from bottom to top curve) of 2.3, 4.5, 5.9, 8.7 and 25.4 μM. Fitted active site concentration is 6.1 μM and K_d = 0.37 μM.

Fluorescence difference spectra, obtained during titration, may be compared to the fluorescence of an equimolar amount of the neutral and anionic forms of the ligand (cf. Fig. 2 and 6). This points to ~ 10-fold increase of the ligand fluorescence upon binding to PNP, assuming that it remains in its neutral form. By contrast, the free anionic form of the ligand is ~ 40-fold more fluorescent than its neutral form (cf. Table I and Fig. 2), and 4- to 5-fold more fluorescent than the complex (not shown). Since quenching of ligand fluorescence is not observed upon association of any purine analogue with calf spleen PNP (Wierzchowski *et al.*, 1999; Wielgus-Kutrowska *et al.*, 2003, and unpublished data), we conclude that, in the complex, the ligand cannot be ionized, but rather that enhancement of the emission of the neutral species (*i.e.* that observed in the pH range 4–7) is observed. This conclusion is supported by the UV difference spectrum recorded during titration (cf. Fig. 7), which clearly does not resemble the difference between the neutral and anionic species of PME-azaG.

In light of the foregoing, the proposed structure of the fluorescent complex of calf spleen PNP with guanine requires re-interpretation. The strong increase in emission observed in this complex (λ_{max} ~ 330 nm), ascribed to the anion of Gua by Porter (1992), may originate from the N(7)H neutral tautomer (cf. Wielgus-Kutrowska *et al.*, 2002). This tautomer was long ago shown to fluoresce strongly in rigid glasses at 140–160 K, with ϕ ~ 0.7 and λ_{max} ~ 325 nm, while the predominant N(9)H form exhibits no fluorescence even under these highly favorable conditions (Wilson and Callis, 1980). Although guanine and N^7-methylguanine do not emit in neutral aqueous medium at room temperature ($\phi < 10^{-3}$), the reported very strong binding of purines by PNP in the absence of phosphate (Kline and Schramm, 1992; Bzowska *et al.*, 2000; Bzowska, 2002) may lead to increased rigidity in the complex, resulting in an enhanced fluorescence yield of the bound neutral N(7)H form, as observed for other weakly fluorescent ligands on binding (Wierzchowski *et al.*, 1999; Wielgus-Kutrowska *et al.*, 2003).

The foregoing supports the Schramm model of the reaction, postulating protonation of the purine ring N(7) as the initial step in nucleoside phosphorolysis (Kline and Schramm, 1995), subsequently also proposed for *E. coli* PNP, where the essential Asp204 residue is presumed to be responsible for nucleoside N(7) protonation in the transition state (Koellner *et al.*, 2002; Bennett *et al.*, 2003). The situation is less clear for mammalian PNPs, where the acidic Glu201, presumably in the anionic state, is located close to the nucleoside N(1)H, and N(7) is bound either to Asn243 or to a structural water molecule (Fedorov *et al.*, 2001). Our results suggest that, in the transition state, the N(7) may be protonated, as it is at the reaction endpoint, although the pathway to this protonation remains unresolved.

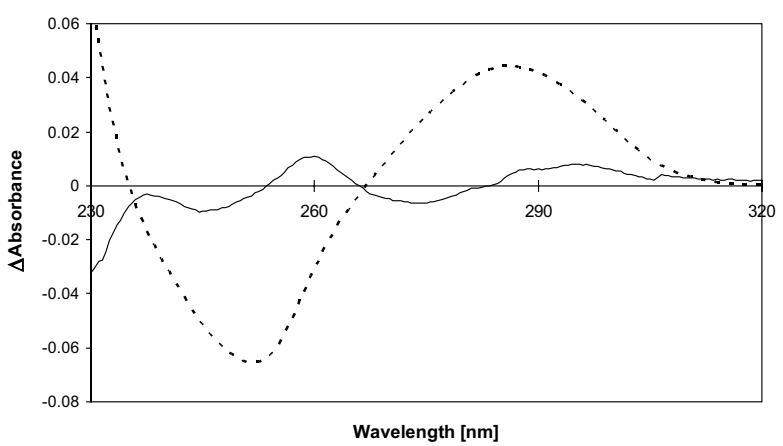

Fig. 7. (———) UV difference spectrum in 20 mM acetate buffer, pH 5.9, between calf spleen PNP (11.9 μM) + 25.44 μM PME-azaG and the sum of the two; (- - - -) calculated difference spectrum between the anionic and neutral forms of PME-azaG (11.9 μM). The terms "anionic" and "neutral" refer to the fluorophore only, and not to the phosphonate moiety.

Acknowledgements

We are indebted to Professor A. Holý for a sample of PME-azaG and to Ms. Lucyna Magnowska for excellent technical assistance. We thank the Department of Chemistry, Faculty of Pharmacy, Warsaw Medical School, for kindly providing access to spectral equipment. This work profited from grants No. 3P04A02425 and 3P04A 03524 from the State Committee for Scientific Research (K. B. N.) and from the University of Podlasie in Siedlce, Poland.

Albert A. (1986), Chemistry of 8-azapurines. Adv. Heterocycl. Chem. **39**, 117–178.

Bennett E. M., Li C., Allan P. W., Parker W. B., and Ealick S. E. (2003), Structural basis for substrate specificity of *E. coli* PNP. J. Biol. Chem. **278**, 47110–47118.

Bzowska A. (2002), Calf spleen purine nucleoside phosphorylase: complex kinetic mechanism, hydrolysis of 7-methylguanosine, and oligomeric state in solution. Biochim. Biophys. Acta **1596**, 293–317.

Bzowska A., Kulikowska E., and Shugar D. (2000), Purine nucleoside phosphorylases: properties, functions and clinical aspects. Pharmacol. Therap. **88**, 349–425.

Deng H., Lewandowicz A., Cahill S. M., Furneaux R. H., Tyler P. C., Girvin M. E., Callender R., and Schramm V. L. (2004), Assignment of downfield proton resonances in purine nucleoside phosphorylase – immucillin-H complex by saturation-transferred NOEs. Biochemistry **43**, 1980–1987.

Erion M. D., Stoeckler J. D., Guida W. C., Walter R. L., and Ealick S. E. (1997), Purine nucleoside phosphorylase. 2. Catalytic mechanism. Biochemistry **36**, 11735–11748.

Fedorov A., Shi W., Kicska G., Fedorov E., Tyler P. C., Furneaux R. H., Hanson J. C., Gainsford G. J., Larese J. Z., Schramm V. L., and Almo S. C. (2001), Transition state structure of purine nucleoside phosphorylase and principles of atomic motion in enzymatic catalysis. Biochemistry **40**, 853–860.

Holý A., Dvorakova H., Jindrich J., Masojidkova M., Budesinsky M., Balzarini J., Andrei G., and De Clercq E. (1996), Acyclic nucleotide analogs derived from 8-azapurines: synthesis and antiviral activity. J. Med. Chem. **39**, 4073–4088.

Iwanow M., Magnowska L., Yokomatsu T., Shibuya S., and Bzowska A. (2003), Interactions of potent multisubstrate analogue inhibitors with purine nucleoside phosphorylase from calf spleen: Kinetic and spectrofluorimetric studies. Nucleosides, Nucleotides and Nucleic Acids **22**, 1567–1570.

Kicska G. A., Tyler P. C., Evans G. B., Furneaux R. H., Schramm V. L., and Kim K. (2002a), Purine-less death in *Plasmodium falciparum* induced by immucillin-H, a transition state analogue of purine nucleoside phosphorylase. J. Biol. Chem. **277**, 3226–3231.

Kicska G. A., Tyler P. C., Evans G. B., Furneaux R. H., Shi W.-X., Fedorov A., Lewandowicz A., Cahill S. M., Almo S. C., and Schramm V. L. (2002b), Atomic dissection of the hydrogen bond network for transition-state analogue binding to purine nucleoside phosphorylase. Biochemistry **41**, 14489–14498.

Kierdaszuk B., Modrak-Wójcik A., Wierzchowski J., and Shugar D. (2000), Formycin A and its N-methyl analogues, specific inhibitors of *E. coli* purine nucleoside phosphorylase: induced tautomeric shift on binding to enzyme, and enzyme → ligand fluorescence resonance energy transfer. Biochim. Biophys. Acta **1476**, 109–128.

Kline P. C. and Schramm V. L. (1992), Purine nucleoside phosphorylase. Inosine hydrolysis, tight binding of the hypoxanthine intermediate, and third-the-sites reactivity. Biochemistry **31**, 5964–5973.

Kline P. C. and Schramm V. L. (1995), Pre-steady-state transition-state analysis of the hydrolytic reaction catalyzed by purine nucleoside phosphorylase. Biochemistry **34**, 1153–1162.

Koellner G., Bzowska A., Wielgus-Kutrowska B., Luić M., Steiner T., Saenger W., and Stępiński J. (2002), Open and closed conformation of the *E. coli* purine nucleoside phosphorylase active center and implications for the catalytic mechanism. J. Mol. Biol. **315**, 351–371.

Kulikowska E., Bzowska A., Wierzchowski J., and Shugar D. (1986), Properties of two unusual, and fluorescent substrates of purine-nucleoside phosphorylase: 7-methylguanosine and 7-methylinosine. Biochim. Biophys. Acta **874**, 355–366.

Kulikowska E., Bzowska A., Holý A., Magnowska L., and Shugar D. (1998), Antiviral acyclic nucleoside phosphonates as inhibitors of purine nucleoside phosphorylase. Adv. Exp. Med. Biol. **431**, 747–752.

Lewandowicz A., Shi W.-X., Evans G. B., Tyler P. C., Furneaux R. H., Basso L. A., Santos D. S., Almo S. C., and Schramm V. L. (2003), Over-the-barrier transition state analogues and crystal structure with *Mycobacterium tuberculosis* purine nucleoside phosphorylase. Biochemistry **42**, 6057–6066.

Mao C., Cook W. J., Zhou M., Federov A. A., Almo S. C., and Ealick S. E. (1998), Calf spleen purine nucleoside phosphorylase complexed with substrates and substrate analogues. Biochemistry **37**, 7135–7146.

Miles R. W., Tyler P. C., Furneaux R. H., Bagdassarian C. K., and Schramm V. L. (1998), One third-the-sites transition-state inhibitors for purine nucleoside phosphorylase. Biochemisty **37**, 8615–8621.

Porter D. J. (1992), Purine nucleoside phosphorylase. Kinetic mechanism of the enzyme from calf spleen. J. Biol. Chem. **267**, 7342–7351.

Pugmire M. J. and Ealick S. E. (2002), Structural analyses reveal two distinct families of nucleoside phosphorylases. Biochem. J. **361**, 1–25.

Sauve A. A., Cahill S. M., Zech S. G., Basso L. A., Lewandowicz A., Santos D. S., Grubmeyer C., Evans G. B., Furneaux R. H., Tyler P. C., McDermott A., Girvin M. E., and Schramm V. L. (2003), Ionic states of substrates and transition state analogues at the catalytic sites of N-ribosyltransferases. Biochemistry **42**, 5694–5705.

Schramm V. L. (2002), Development of transition state analogues of purine nucleoside phosphorylase as anti-T-cell agents. Biochim. Biophys. Acta **1587**, 107–117 (and references cited therein).

Segel I. H. (1975), Enzyme Kinetics. J. Wiley and Sons, New York.

Shugar D. and Psoda A. (1991), Tautomerism of purines and pyrimidines, their nucleosides and various analogues. In: Landoldt-Bornstein Encyclopedia on Numerical Data and Functional Relationships in Science and Technology, Vol. VII/1d (Madelung O., ed.). Springer, Berlin, pp. 308–348.

Tebbe J., Bzowska A., Wielgus-Kutrowska B., Kazimierczuk Z., Schröder W., Shugar D., Saenger W., and Koellner G. (1999), Crystal structures of purine nucleoside phosphorylase (PNP) from *Cellulomonas* sp. and its implications for the molecular mechanism of trimeric PNPs. J. Mol. Biol. **294**, 1239–1255.

Wielgus-Kutrowska B., Bzowska A., Tebbe J., Koellner G., and Shugar D. (2002), Purine nucleoside phosphorylase from *Cellulomonas* sp.: physicochemical properties and binding of substrates determined by ligand-dependent enhancement of enzyme intrinsic fluorescence, and by protective effects of ligands on thermal inactivation of the enzyme. Biochim. Biophys. Acta **1597**, 320–334.

Wielgus-Kutrowska B., Frank J., Holý A., Koellner G., and Bzowska A. (2003), Interactions of trimeric purine nucleoside phosphorylases with ground state analogues: Calorimetric and fluorimetric studies. Nucleosides, Nucleotides and Nucleic Acids **22**, 1695–1698.

Wierzchowski J., Wielgus-Kutrowska B., and Shugar D. (1996), Fluorescence emission properties of 8-azapurines and their nucleosides, and application to the kinetics of the reverse synthetic reaction of purine nucleoside phosphorylase. Biochim. Biophys. Acta **1290**, 9–17.

Wierzchowski J., Kulikowska E., Bzowska A., Holý A., Magnowska L., and Shugar D. (1999), Interactions of purine nucleoside phosphorylase with antiviral acyclic nucleoside phosphonate inhibitors – kinetic and emission studies. Nucleosides Nucleotides **18**, 875–876.

Wierzchowski J., Ogiela M., Iwańska B., and Shugar D. (2002), Selective fluorescent and fluorogenic substrates for purine-nucleoside phosphorylases from various sources, and direct fluorimetric determination of enzyme levels in human and animal blood. Anal. Chim. Acta **472**, 63–74.

Wilson M. and Callis P. R. (1980), Prototropic tautomerism and the apparent photophysics of adenine and guanine at 77 K. Photochem. Photobiol. **31**, 323–327.